

Rapidly Spinning Black Holes in Quasars: An Open Question

Alireza Rafiee, Patrick B. Hall

Department of Physics & Astronomy, York University, Toronto, Ontario M3J 1P3, Canada

ABSTRACT

Wang et al. (2006) estimated an average radiative efficiency of 30%–35% for quasars at moderate redshift. We find that their method is not independent of quasar lifetimes and thus that quasars do not necessarily have such high efficiencies. Nonetheless, it is possible to derive interrelated constraints on quasar lifetimes, Eddington ratios, and radiative efficiencies of supermassive black holes. We derive such constraints using a statistically complete sample of quasars with black hole mass estimates from broad Mg II. For quasars with $L/L_{Edd} \gtrsim 1$, lifetimes can range from 60 Myr for the nonrotating case to 460 Myr for the maximally rotating case. Coupled with observed black hole masses, long quasar lifetimes would imply high radiative efficiencies while quasar lifetimes of ≤ 60 Myr would imply that radiatively inefficient accretion must be important in the accretion history of quasars.

Subject headings: black hole physics — quasars: general

1. Introduction

A quasar is powered by matter accreting onto a supermassive black hole (e.g., Rees 1984). Gas orbiting in the innermost stable circular orbit (ISCO) may be perturbed and fall into the black hole (BH), adding mass and angular momentum to it. To have reached the ISCO *through a thin accretion disk*, gas must have radiated away a fractional binding energy per unit rest mass $\simeq 1 - (1 - 2GM/3c^2 R_{ISCO})^{1/2}$ which is the system's *radiative efficiency* η (Bardeen 1970). Since R_{ISCO} decreases from $6GM/c^2$ for Schwarzschild (nonrotating) BHs to GM/c^2 for co-aligned accretion onto Extreme-Kerr (maximally rotating) BHs, more energy is produced by (co-aligned) thin disk accretion of a given mass onto a rotating BH than onto a non-rotating BH (Carter 1968).

If a quasar accretes gas with a fixed angular momentum vector at a fixed mass accretion rate \dot{M} , the BH spin will increase to a theoretical maximum and the luminosity L of the quasar will increase along with it, since $L \propto \eta \dot{M} c^2$. In many realistic accretion models,

the spin of a supermassive BH increases rapidly and then fluctuates around a maximum value, although spin-down is also possible (Volonteri 2007). Several such models, including numerical ones by Di Matteo et al. (2005), suggest that the accretion process stops when a BH becomes massive enough to support a kinetic and/or radiative luminosity capable of blowing away the gas fuelling it (Silk & Rees 1998; Fabian 1999; King 2003). However, the radiative luminosity for a given mass accretion rate depends upon the radiative efficiency. A rapidly rotating BH can help shut down the accretion process earlier than a nonrotating BH could. Knowledge of supermassive BH spins is therefore useful in constraining models of quasar development.

Observationally, the quasi-periodic variability detected in Sgr A* may be evidence of rapid spin of the Galactic BH (e.g., Genzel et al. 2003). Evidence for rotating supermassive BHs comes from studies of X-ray Fe K α line profiles (Blandford et al. 1990) and by theoretical arguments that powerful radio jets are powered by the extraction of energy from rotating BHs (Miller 2007).

In a recent study, Wang et al. (2006; hereafter WCHM) estimated a high average radiative efficiency of 30%–35% for quasars at $0.4 < z < 2.1$, implying that most supermassive black holes are rapidly rotating. However, the existence of rotating BHs with $\eta \gtrsim 0.18$ is not confirmed by magnetohydrodynamic (MHD) simulations: gas loses more angular momentum prior to accretion in an MHD disk than in a standard thin disk (Gammie & Shapiro 2004; Shapiro 2005). Observationally, Shankar et al. (2008) present and review evidence for $\eta \lesssim 0.1$. In this work we show that the WCHM method is not independent of quasar lifetimes. In § 2 we correct and extend the WCHM method for determining radiative efficiencies, in § 3 we apply it to a sample of Sloan Digital Sky Survey (SDSS) quasars and in § 4 we discuss our conclusions.

2. The Method

We assume that quasar light derives only from accretion of matter onto a black hole, neglecting the effects of BH mergers. Suppose that mass propagates through a thin accretion disk around an accreting BH at a rate of \dot{M}_{acc} during some time interval of Δt .

The BH mass growth rate is given by $\dot{M} = (1 - \eta)\dot{M}_{acc}$, where η is the radiative efficiency. The quasar radiates at bolometric luminosity L (Marconi et al. 2004) given by:

$$L\Delta t = \eta\dot{M}_{acc}c^2\Delta t = \frac{\eta}{1 - \eta}\dot{M}c^2\Delta t. \quad (1)$$

We can rewrite the above equation as:

$$\eta = \frac{L\Delta t}{L\Delta t + \dot{M}c^2\Delta t} \equiv \frac{\delta\epsilon}{\delta\epsilon + \delta\rho c^2} \quad (2)$$

where $\delta\epsilon \equiv L\Delta t/V_{com}$ is the change over the time Δt in the comoving radiative energy density and $\delta\rho \equiv \dot{M}\Delta t/V_{com}$ is the accompanying change in the comoving BH mass density, both due solely to this BH's accretion.

By analogy, an average radiative efficiency can be defined for any sample of quasars at redshift z :

$$\bar{\eta}(z) \equiv \frac{\Delta\epsilon(z)}{\Delta\epsilon(z) + \Delta\rho(z)c^2} \quad (3)$$

where $\Delta\epsilon(z)$ and $\Delta\rho(z)$ are the changes in the *cumulative* radiative energy density and the *cumulative* mass density of the sample in the redshift range $(z, z + \Delta z)$. We now define these cumulative densities.

We require the quasar black hole mass function $n(M, z)$, defined such that $n(M, z) \Delta M \Delta z$ is the comoving number density of black holes with masses in the range $(M, M + \Delta M)$ in the redshift range $(z, z + \Delta z)$. We also require the quasar bolometric luminosity function $\psi(L, z)$, where $\psi(L, z) \Delta L \Delta z$ is the comoving number density of black holes with bolometric luminosity in the range $(L, L + \Delta L)$ in the redshift range $(z, z + \Delta z)$.

Over its lifetime t_q , a single quasar accretes a mass $M_{final} = \dot{M}_{avg} t_q$ and radiates an energy $L_{avg} t_q$. We need to express those quantities in terms of the observables M_i and L_j , which are the black hole's mass and bolometric luminosity at the redshift of observation, z . We do so by defining correction factors \bar{f} and \bar{g} such that

$$\bar{f} = \frac{1}{N} \sum_{i=1}^N \frac{M_i}{M_{final,i}} = \left\langle \frac{M_i}{M_{final,i}} \right\rangle \quad \text{and} \quad \bar{g} = \frac{1}{N} \sum_{j=1}^N \frac{L_j}{L_{avg,j}} = \left\langle \frac{L_j}{L_{avg,j}} \right\rangle \quad (4)$$

where the averages are over all N quasars in the sample.

First, consider the mass density that contributes to Eq. 3. Over their lifetimes, all black holes observed at redshift z will accrete a comoving matter density of

$$\sum_{M_i} n(M_i, z) M_{final} \Delta M_i = \sum_{M_i} n(M_i, z) M_i \Delta M_i / \bar{f}. \quad (5)$$

The cumulative, lifetime amount of matter accreted by all black holes observed at $\geq z$ and above is the comoving lifetime mass density summed over all redshifts $\geq z$:

$$\varrho(z) = \sum_{z_k \geq z} \Delta\varrho(z_k) = \sum_{z_k \geq z} \Delta z_k \sum_{M_i} n(M_i, z_k) M_i \Delta M_i / \bar{f} \quad (6)$$

which agrees with Eqs. 2 and 6 of WCHM if $\bar{f} = 1$. Units of $\Delta\varrho/\Delta z$ are mass per comoving volume per redshift.

Now consider the radiative energy component of Eq. 3. Over their lifetimes, all black holes observed at redshift z will radiate a comoving energy density of

$$\sum_{L_j} \psi(L_j, z) L_{avg} \bar{t}_q \Delta L_j = \sum_{L_j} \psi(L_j, z) L_j \bar{t}_q \Delta L_j / \bar{g}, \quad (7)$$

where \bar{t}_q is the average quasar lifetime.¹ The cumulative, lifetime amount of energy radiated by all black holes observed at redshift z and above is the comoving lifetime energy density summed over all redshifts above z :²

$$\varepsilon(z) = \sum_{z_k > z} \Delta\varepsilon(z_k) = \sum_{z_k > z} \Delta z_k \sum_{L_j} \psi(L_j, z_k) L_j \bar{t}_q \Delta L_j / \bar{g} \quad (8)$$

which differs from Eqs. 3 and 5 of WCHM. Their expression for $\Delta\varepsilon(z)$ is a factor of $\Delta t_k / \Delta z_k \bar{t}_q$ times the true value above (assuming $\bar{g} = 1$), where Δt_k is the cosmological time spanned by the redshift interval Δz_k . The units of $\Delta\varepsilon/\Delta z$ above are energy per comoving volume per redshift, whereas in Eq. 5 of WCHM they are energy per comoving volume per (redshift)², which is incorrect.

Thus, the change in the *cumulative* comoving mass density of actively accreting black holes over the redshift range $(z, z + \Delta z) - \Delta\varrho(z)$ — is Δz times the sum of the masses of all individual quasar black holes in the sample in that z range, divided by the comoving volume:

$$\Delta\varrho(z) = \Delta z \sum_{M_i} n(M_i, z) M_i \Delta M_i / \bar{f}. \quad (9)$$

In other words, the rate of change in the *cumulative* comoving mass density in the redshift bin $(z, z + \Delta z) - \Delta\varrho(z)/\Delta z$ — is the same as the comoving mass density in that bin. Similarly, the change over the redshift range $(z, z + \Delta z)$ in the cumulative radiative energy

¹ Time periods without accretion are not counted in \bar{t}_q . While \bar{t}_q can be defined as the sum of all time periods during which an average quasar is actively accreting mass, an acceptable observational definition might be the time required to accrete, e.g., 95% of the quasar’s final mass (see Hopkins et al. 2006).

²For convenience, in Equations 6 and 8 the redshift sum appears in front of the mass or luminosity sum for that redshift bin. That latter sum is computed in the k th redshift bin, multiplied by Δz_k and then added to the mass or luminosity sum from the $(k+1)$ th redshift bin times Δz_{k+1} , and so on. The redshift bin size does not matter as long as $n(M, z_k)$ or $\psi(L_j, z_k)$ does not change considerably within a bin. For example, if the redshift bin width was halved, each term in the redshift sum would be half as large but there would be twice as many terms, yielding the same result.

density ever observed from all quasars — $\Delta\varepsilon(z)$ — is

$$\Delta\varepsilon(z) = \Delta z \sum_{L_j} \psi(L_j, z) L_j \Delta L_j \bar{t}_q / \bar{g}. \quad (10)$$

These expressions for $\Delta\rho(z)$ and $\Delta\varepsilon(z)$ can be substituted into Eq. 3 to find $\bar{\eta}(z)$ for the sample of quasars under consideration. Doing so, and grouping the constants \bar{t}_q , \bar{f} and \bar{g} together, we obtain:

$$\bar{\eta}(z) = \frac{\sum_{L_j} \psi(L_j, z) L_j \Delta L_j}{\sum_{L_j} \psi(L_j, z) L_j \Delta L_j + \frac{\bar{g}c^2}{\bar{f}\bar{t}_q} \sum_{M_i} n(M_i, z) M_i \Delta M_i} \quad (11)$$

where the Δz in the numerator and denominator have cancelled out, making the calculation independent of Δz .

Thus, the WCHM method for studying radiative efficiencies is not independent of the average quasar lifetime \bar{t}_q . A factor of \bar{t}_q enters because both the mass-energy growth and the radiative energy output of a quasar must be summed over its entire lifetime (or over the same portion of its lifetime). The mass-energy sum yields the final mass-energy of the black hole $M_{tot}c^2$, while the radiative energy sum yields $L_{avg}\bar{t}_q$. However, this method remains independent of obscured sources, and is also powerful because it can be implemented for any sample of quasars regardless of selection effects. It requires only that the changes in the cumulative mass-energy and radiative energy densities be computed using the same objects. Of course, selection effects *will* determine if the resulting radiative efficiency is relevant for quasars in general.

In effect, WCHM assumed $\bar{f} = \bar{g} = 1$. More realistic estimates can be found by examining Fig. 1 of Hopkins et al. (2005) and Fig. 14 of Springel et al. (2005), from which we estimate $\bar{f} \simeq 1$ and $\bar{g} \simeq 3$ for those models. (If WCHM had assumed $\bar{f} = 1$ and $\bar{g} = 3$, we estimate that their (incorrect) calculation would have yielded $\eta \simeq 0.14$ instead of $\eta \simeq 0.32$.) However, Eq. 11 shows that even with realistic \bar{f} and \bar{g} values the average quasar radiative efficiency is dependent on the average quasar lifetime. We now explore the implications of this dependency.

3. Application to SDSS Quasars

3.1. Estimation of Black Hole Masses

Based on reverberation mapping studies of local active galaxies, an empirical scaling relationship has been developed to estimate black hole masses by (e.g.) Kaspi et al. (2000), Vestergaard (2002) and McLure et al. (2002). The Sloan Digital Sky Survey (York et al. 2000) Data Release 3 quasar catalog (Schneider et al. 2005) provides us with a large sample of quasars at redshifts $0.7 < z < 2.1$ which have their Mg II $\lambda 2800$ emission line redshifted into the SDSS spectral range. We have estimated black hole masses for 27728 such quasars from the dispersion of the Mg II emission line and the continuum luminosity at $\lambda=3000$ Å via the relationship $M_{BH}/M_{\odot} = 30.5[\lambda L_{\lambda}]^{0.5} \sigma_{Mg}^2$ where L_{λ} has units of 10^{44} erg s⁻¹ and σ_{Mg} km s⁻¹ (Rafiee et al. 2008, in prep.).

3.2. Black Hole Mass and Luminosity Functions

We have matched our sample with that of Richards et al. (2006a), a homogeneously selected and statistically complete sample of 15343 DR3 quasars with redshifts $z < 5$ drawn from an effective area of 1622 deg². This procedure yields a subsample of 8809 quasars. The bolometric luminosities of these quasars have been estimated from $L_{bol} = C_{\nu} \nu L_{\nu}$ with $C_{\nu} = 5$ (Fig. 12 of Richards et al. 2006b) for $\nu = c/2500$ Å and $\log(L_{\nu}) = 20.16 - 0.4M_i(z = 2)$ (Richards et al. 2006a). Comoving volumes and luminosity distances have been calculated using a cosmology with $h = 0.7$, $\Omega_{\Lambda} = 0.7$ and $\Omega_m = 0.3$. Corrections have been made for the limited areal coverage of the Richards et al. (2006a) sample and for the 5% incompleteness of the SDSS at $0.7 < z < 2.1$. For more details, see Fig. 8 of Richards et al. (2006a).

3.3. Redshift Binning

For a thin accretion disk, η varies from 0.057 for a Schwarzschild BH (with $a^* \equiv Jc/GM^2 = 0$, where J is the angular momentum) to 0.42 for an Extreme-Kerr BH ($a^* = 1$). When one takes into account the effect of radiation energy captured by the BH (Thorne 1974), the radiative efficiency reaches a maximum of $\simeq 0.30$ ($a^* \simeq 0.998$); we refer to that case as a Thorne BH. It is more realistic to assume an MHD disk wherein magnetic turbulence provides a torque to remove angular momentum from the inflowing gas (Shapiro 2005);

in that case, the maximum radiative efficiency is $\simeq 0.18$ ($a^* \simeq 0.938$).³

We divide our sample into twelve redshift bins. In each bin we can compute η for any given value of \bar{t}_q . The results are shown in Figure 1 as tracks of $\eta(z)$ for eight different values of \bar{t}_q chosen to match the η of a Schwarzschild, MHD, Thorne or Extreme-Kerr black hole at either the high or low redshift limit of our sample. Figure 1 is comparable to Figure 2 of WCHM. Both figures show the evolution of η with z for a flux-limited quasar sample, *assuming* constant \bar{t}_q . However, neither figure gives the complete picture since there is another degree of freedom not considered in such figures; namely, the Eddington ratios of the quasars. For example, taken at face value, Figure 1 suggests that a quasar powered by a Thorne BH can live for 0.26 Gyr at $z \simeq 2$ but for 0.54 Gyr at $z \simeq 0.8$. However, quasars in our sample have larger values of the Eddington ratio at $z \simeq 2$ than at $z \simeq 0.8$, so the trend in Figure 1 may be with Eddington ratio rather than with redshift. To investigate this possibility, we bin quasars in Eddington ratio as well as redshift.

3.4. Eddington Ratio Binning

We assume the radiative efficiency may be a function of the Eddington ratio $\Upsilon \equiv L_{bol}/L_{Edd}$, where $L_{Edd} = 1.26 \times 10^{38} (M_{BH}/M_\odot) \text{ erg s}^{-1}$. In that case, the changes in the *cumulative* comoving mass and energy densities in the Eddington ratio bin $(\Upsilon, \Upsilon + \Delta\Upsilon)$ are:

$$\Delta\rho_\bullet(z, \Upsilon) = \Delta\Upsilon \Delta z \sum_{M_i} n(\Upsilon, M_i, z) M_i \Delta M_i / \bar{f}. \quad (12)$$

$$\Delta\varepsilon_\bullet(z, \Upsilon) = \Delta\Upsilon \Delta z \sum_{L_j} \psi(\Upsilon, L_j, z) L_j \Delta L_j \bar{t}_q / \bar{g} \quad (13)$$

where n and ψ now depend on Υ as well as z . The bullet subscript denotes quantities binned in Υ as well as z . The average radiative efficiency for a given Υ and z is

$$\bar{\eta}(z, \Upsilon) = \frac{\Delta\varepsilon_\bullet(z, \Upsilon)}{\Delta\varepsilon_\bullet(z, \Upsilon) + \Delta\rho_\bullet(z, \Upsilon)c^2}. \quad (14)$$

For the same sub-sample used in section 3.2 and for twelve redshift bins, ten mass bins, and ten luminosity bins, the radiative efficiency has been estimated for six different Eddington

³We relate η to a^* assuming co-aligned accretion on to rotating BHs. King, Pringle & Hofmann (2008) have pointed out that the effective $\eta(a^*)$ will be different for randomly-aligned accretion. The conversion from η to a^* will differ for each combination of co- and randomly-aligned accretion, but high η will always require high a^* .

ratios (Figure 2). Because the sample is flux-limited, there are few quasars with low Eddington ratios in the high- z bins (Figure 2a) and few super-Eddington objects in the low- z bins (Figure 2f), making the uncertainties very large in those bins. Figure 2 shows that *radiative efficiency is not a function of redshift but rather of quasar lifetime and Eddington ratio*.

4. Discussion and Summary

Determinations of quasar lifetimes, Eddington ratios and radiative efficiencies are inter-related. Given constraints on (or assumptions about) quasar lifetimes, the WCHM method can be used to constrain quasar radiative efficiencies and BH spins. (*Without such constraints, the average quasar η cannot be estimated by this method.*) Conversely, the range of radiative efficiencies possible for the full range of BH spins can be used to constrain average quasar lifetimes, as long as luminous quasars are not powered by radiatively inefficient accretion flows (RIAFs; see, e.g., Blandford & Begelman 1999). For example, for both the $\eta = 0.065, \Upsilon \simeq 0.4$ and $\eta = 0.09, \Upsilon \simeq 0.9$ models of Shankar et al. (2008), we predict $\bar{t}_q \simeq 0.2$ Gyr, which could be used as a further test of those models in comparison to others.

Assuming $\bar{f} = 1$ and $\bar{g} = 3$ (see the end of § 2), quasar lifetimes can be constrained according to the Eddington ratio of the quasar. Lifetimes estimated this way are within a factor of a few of literature lifetime estimates. For example, for BHs in the mass range of our sample ($10^8 < M_{BH} < 10^9 M_\odot$), a lower limit lifetime of 0.55 billion years can be established for black holes with $0.02 < \Upsilon < 0.2$ (Figure 2a). This lower limit corresponds to the Schwarzschild case, since a rotating black hole at the same Υ will require a longer lifetime to build up its observed mass. This lower limit lifetime is only a factor of two lower than the mean lifetime of one billion years estimated by Marconi et al. (2004) for $\Upsilon = 0.1$ and $\eta = 0.04$ in the same range of M_{BH} . As another example, a luminous quasar powered by a relatively low-mass black hole — which may be a typical early stage in a quasar’s evolution — will have $\Upsilon \gtrsim 1$ and can have a typical lifetime of 60 to 460 million years (Figure 2f). This range is only a factor of ~ 2.5 larger than the mean lifetime of 30 – 130 million years estimated by Yu & Tremaine (2002) for luminous quasars, and is consistent with the mean lifetime of 100 – 450 million years estimated by Marconi et al. (2004) for super-Eddington accretors.

In principle, given constraints on $\Upsilon \propto \dot{M}/(1 - \eta)M_{BH}$, \bar{f}/\bar{g} and \bar{t}_q for quasar samples, one could estimate the historical frequency of RIAF episodes in those quasars by plotting quasar lifetimes versus Eddington ratios. For example, consider quasars lying below the Schwarzschild curves in Figure 3 (the normalization of which is a function of \bar{f}/\bar{g} , as seen by comparing the two panels). Above our lower mass limit of $10^8 M_\odot$, such quasars must either have had a RIAF phase in order to explain their observed masses, or they must have

observed Eddington ratios lower than their historical average: $\Upsilon_{obs} < \bar{\Upsilon}$. (In the latter case, the quasars historically would have been located horizontally to the right in the diagram, lying between the Schwarzschild and Thorne curves at a value of $\Upsilon = \bar{\Upsilon}$ sufficient to yield the observed M_{BH} in the observed \bar{t}_q .) Conversely, quasars lying above the Thorne curves in Figure 3 require $\Upsilon_{obs} > \bar{\Upsilon}$. A low $\bar{\Upsilon}$ might result if the BH spin does not increase as fast as the BH mass does, perhaps due to counter-rotating gas accretion phases. If $\bar{f} = 1$ and $\bar{g} = 3$ and $\bar{t}_q < 1$ Gyr, and if RIAFs are unimportant, then not many BHs with $\Upsilon < 1$ can be rapidly spinning. On the other hand, if $\bar{f} = 1$ and $\bar{g} = 3$ and $\bar{t}_q < 60$ Myr, then RIAFs must be an important phase for quasars regardless of Υ , since only then could the observed masses be reached in the inferred lifetimes.

REFERENCES

- Bardeen, J. M. 1970, *Nature*, 226, 64.
- Blandford, R. D., Netzer, H., Woltjer, L. Courvoisier, T. J.-L., & Mayor, M. 1990, *Active Galactic Nuclei* (Berlin: Springer-Verlag)
- Blandford, R. D. & Begelman, M. C. 1999, *MNRAS*, 303, L1
- Carter, B. 1968, *Phys. Rev.*, 1559
- Di Matteo, T., Springel, V. & Hernquist, L. 2005, *Nature*, 433, 604
- Fabian, A. C. 1999, *MNRAS*, 308, L39
- Gammie, C., Shapiro, S. & McKinney, J. 2004, *ApJ*, 602, 312
- Genzel, R., et al. 2003, *Nature*, 425, 934
- Hopkins, P. F., et al. 2005, *ApJ*, 625, L71
- Hopkins, P. F., et al. 2006, *ApJ*, 643, 641
- Kaspi, S., Smith, P. S., Netzer, H., et al. 2000, *ApJ*, 533, 631
- King, A. 2003, *ApJ*, 596, L27
- King, A., Pringle, J., Hofmann, J. 2008, *MNRAS*, in press
- Marconi, A., Risaliti, G., et al. 2004, *MNRAS*, 351, 169
- McLure, R. J. & Jarvis, M. J. 2002, *MNRAS*, 337, 109
- Miller, J. M. 2007, *ARA&A*, in press (arXiv:0705.0540)
- Rees, M. J. 1984, *ARA&A*, 22, 471
- Richards, G. T., et al. 2006a, *AJ*, 131, 2766
- Richards, G. T., et al. 2006b, *ApJS*, 166, 470
- Schneider, D. P., et al. 2005 *ApJ*, 130, 367
- Shankar, F., Weinberg, D. & Miraldi-Escude, J. 2008, submitted
- Shapiro, S. L. 2005 *ApJ*, 620, 59

- Silk, J. & Rees, M. J. 1998, A&A 331, L1
- Springel, V., et al. 2005, MNRAS, 361, 776
- Thorne, K. S. 1974, ApJ, 191, 507
- Vestergaard, M. 2002, ApJ, 571, 733
- Volonteri, M. 2007, arXiv:0709.1722
- Wang, J., Chen, Y., Ho, L. & McLure, R. 2006, 642, L111 [WCHM]
- York, D. G., et al. 2000, AJ, 120, 1579
- Yu, Q. & Tremaine, S. 2002, MNRAS, 335, 965

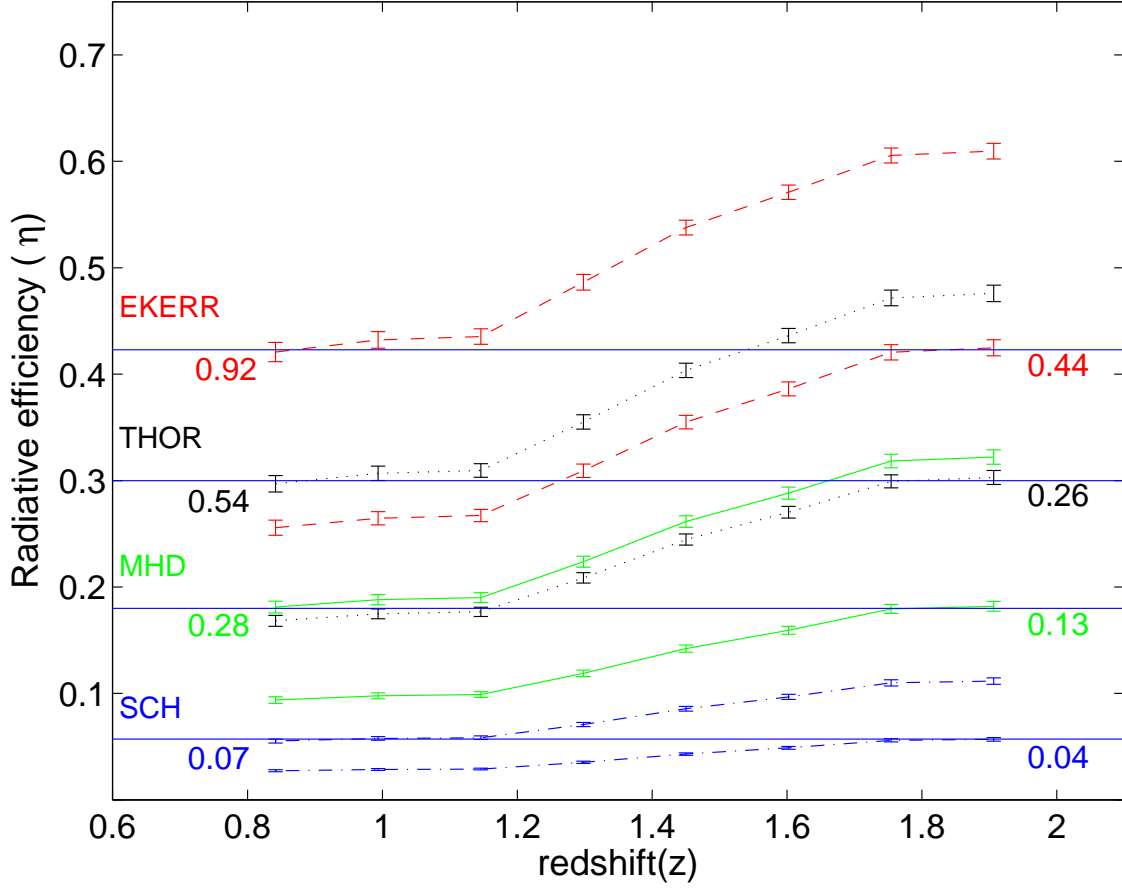


Fig. 1.— Tracks of radiative efficiency vs. redshift for different assumed values of the quasar lifetime in Gyr, all assuming $\bar{f} = \bar{g} = 1$. Red dashed lines are for the Extreme-Kerr BH limit (EKERR), black dotted lines for the Thorne BH limit (THOR), green solid lines for the magnetohydrodynamic BH limit (MHD) and blue dash-dotted lines for the Schwarzschild BH limit (SCH). Estimated quasar lifetimes are given next to each line, on the left for low redshift epochs and on the right for high redshift epochs.

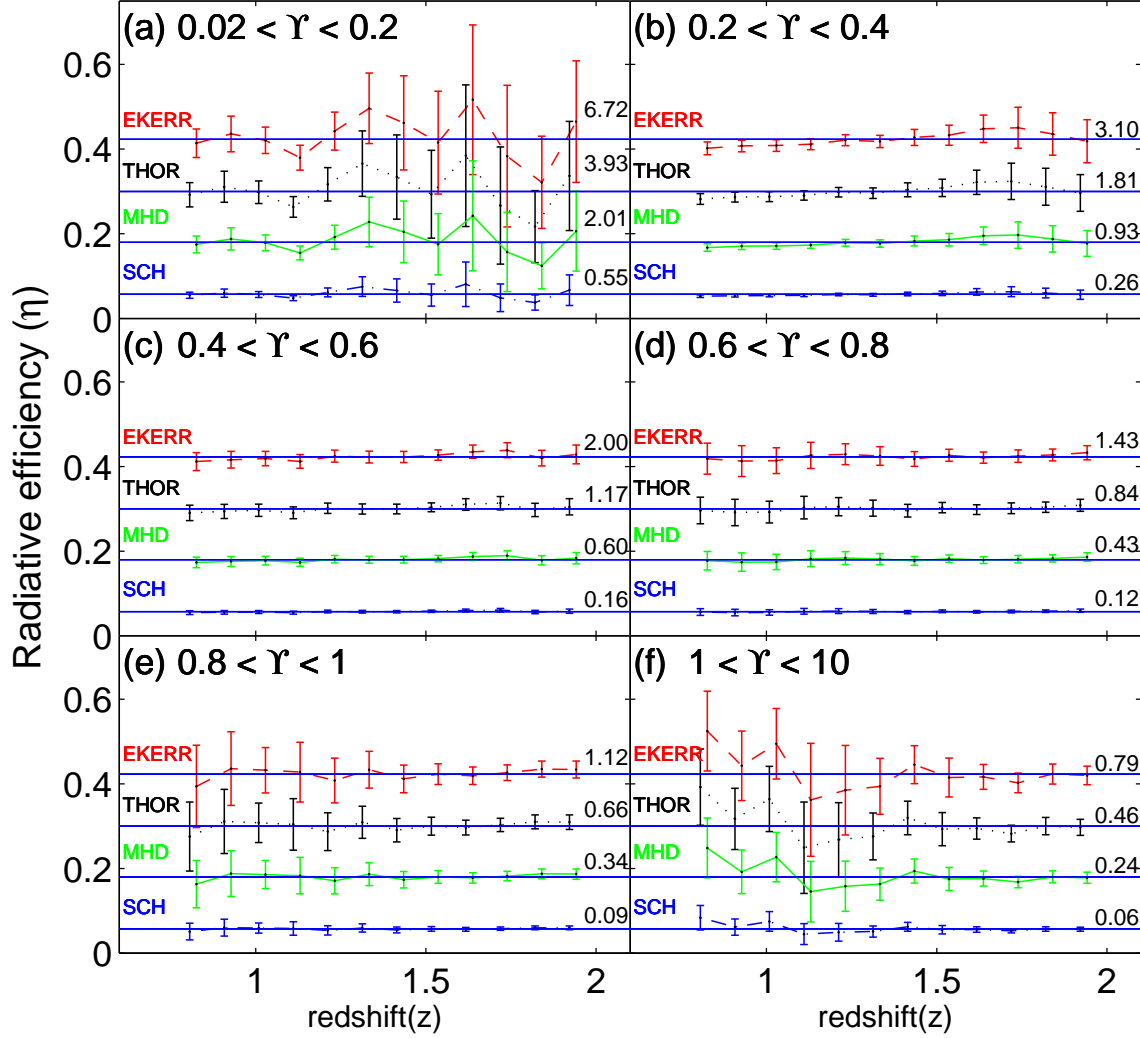


Fig. 2.— Radiative efficiencies vs. z for different Eddington ratio bins and constant assumed quasar lifetimes in Gyr (printed in each panel for each BH type). Lifetimes were chosen so the resulting η would match that of each BH type. We assume $\bar{f} = 1$ and $\bar{g} = 3$ — quasars are observed at their final mass and three times their average luminosity. The color/line codes are the same as in Fig. 1.

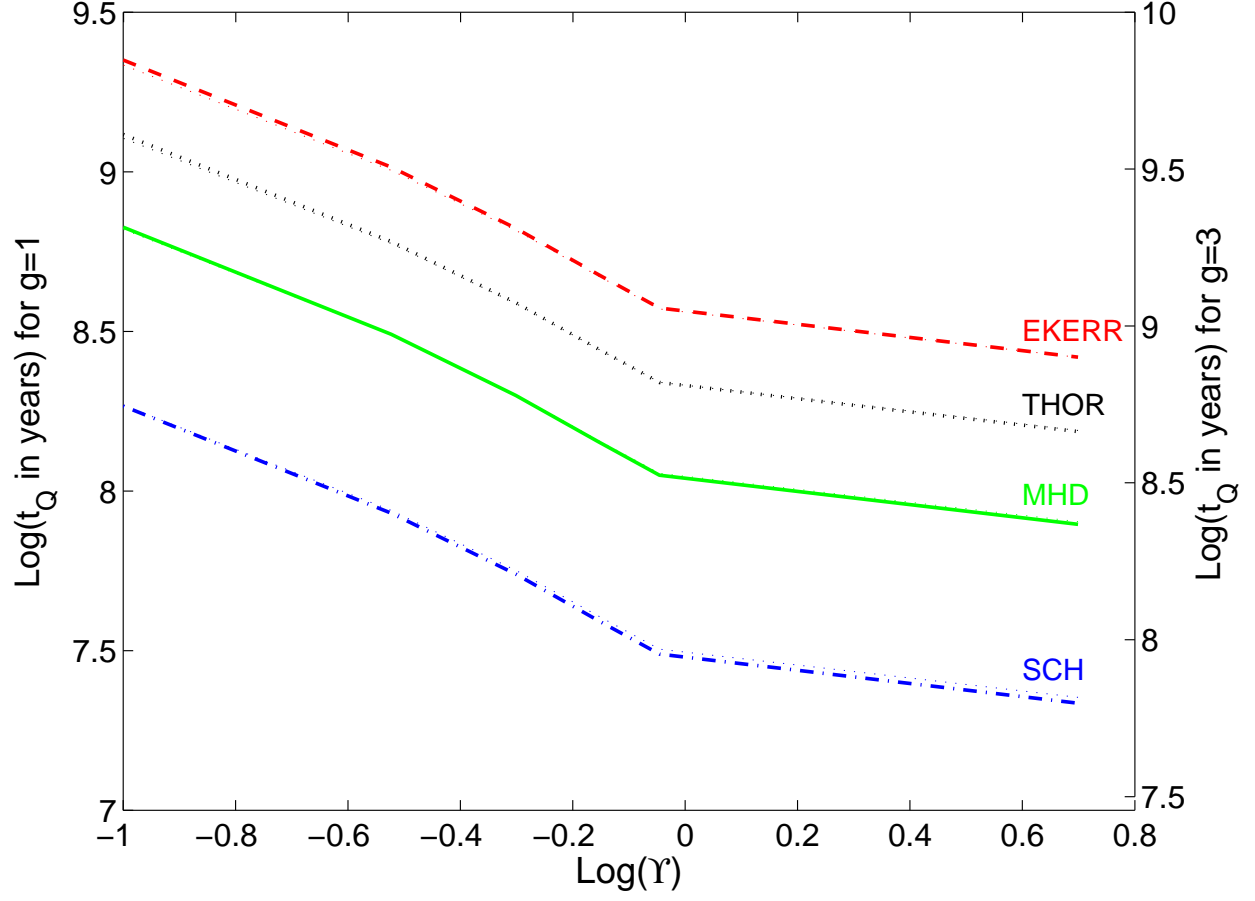


Fig. 3.— Quasar lifetime versus Eddington ratio. Quasars will lie in the area between the Schwarzschild and Thorne curves if they are described by radiatively efficient accretion disks. Below the Schwarzschild curves requires radiatively inefficient accretion or $\tilde{\Upsilon} > \Upsilon_{obs}$, while above the MHD curves requires $\tilde{\Upsilon} < \Upsilon_{obs}$. Left axis labels are for $\bar{f} = \bar{g} = 1$; right axis labels are for $\bar{g} = 3$ and $\bar{f} = 1$. The color/line codes are the same as in Fig. 1.